Title

Ion Transport in Dynamic Polymer Networks Based on Metal-Ligand Coordination: Effect of Cross-Linker Concentration

Journal

Macromolecules, 51(5)

ISSN

0024-9297 1520-5835

Authors

Sanoja, Gabriel E
Schauser, Nicole S
Bartels, Joshua M
et al.

Publication Date

2018-02-27

DOI

10.1021/acs.macromol.7b02141

Peer reviewed

Ion Transport in Dynamic Polymer Networks based on Metal-Ligand Coordination: Effect of Crosslinker Concentration

Gabriel E. Sanoja,[1,2,†,‡] Nicole S. Schauser,[3,‡] Joshua M. Bartels,[2] Christopher M. Evans,[2,§] Matthew E. Helgeson,[2] Ram Seshadri,[3] and Rachel A. Segalman[2,3,]*

[1]Department of Chemical and Biomolecular Engineering, University of California, Berkeley, California, 94720, United States

[2]Department of Chemical Engineering and [3]Materials Department, University of California, Santa Barbara, California, 93106, United States

[*]Email address: segalman@ucsb.edu

Abstract

The development of high-performance ion conducting polymers requires a comprehensive multi-scale understanding of the connection between ion-polymer associations, ionic conductivity, and polymer mechanics. We present polymer networks based on dynamic metal-ligand coordination as model systems to illustrate this relationship. The molecular design of these materials allows for precise and independent control over the nature and concentration of ligand and metal, which are molecular properties critical for bulk ion conduction and polymer mechanics. The model system investigated, inspired by polymerized ionic liquids, is composed of poly(ethylene oxide) with tethered imidazole moieties that facilitate dissociation upon incorporation of nickel (II) bis(trifluoromethylsulfonyl)imide. Nickel-imidazole interactions physically crosslink the polymer, increase the number of elastically active strands, and dramatically enhance the modulus. In addition, a maximum in ionic conductivity is observed due to the competing effects of increasing ion concentration and decreasing ion mobility upon network formation. The simultaneous enhancement of conducting and mechanical properties within a specific concentration regime demonstrates a promising pathway for the development of mechanically robust ion conducting polymers.

Introduction

Polymer networks with dynamic junctions are an important class of materials based on non-covalent interactions such as hydrogen bonds,[1, 2] electrostatic forces,[3, 4] metal-ligand coordination,[5, 6] host-guest complexation,[7, 8] van der Waals forces,[9] and protein associations[10]. In contrast to their permanently crosslinked counterparts, dynamic polymer networks have physical associations with relatively weak binding energies (*i.e.*, $\approx k_B T$) so that thermal fluctuations or external stimuli enable breakage and reformation on time scales suitable for engineering materials.[11, 12] Dynamic polymer networks find numerous applications in energy conversion and storage,[13] thermoplastics,[14] and medicine[15] due to the toughness provided by the energy-dissipating physical associations.[16-18] Given that the lability of physical associations is intimately coupled to the time-dependent bulk properties of dynamic polymer networks, it is essential to understand their role in polymer relaxation mechanisms on timescales relevant to the design of high-performance functional materials.

Dynamic polymer networks exhibit distinct viscoelastic behavior compared to polymer melts.[12, 19, 20] Under deformation these materials behave as elastic rubbers at times shorter than the lifetime of a physical crosslink, but exhibit liquid flow on longer timescales because of microscopic polymer chain diffusion enabled by the breakage of a few crosslinks. The resulting linear viscoelastic response is characterized by longer terminal relaxation times and an increase in plateau modulus relative to polymer melts. Pioneering work on model poly(4-vinylpyridine) crosslinked with *N,C,N*-pincer Pd (II) and Pt (II) complexes demonstrates that the low strain, frequency-dependent dynamic moduli are dictated by the dissociation rate of physical associations as determined by NMR spectroscopy in dilute solution.[6, 21] This and complementary investigations on hydrogels with coiled-coils,[22] bis(histidine)-Ni^{2+},[23, 24] and hydrazone[25] crosslinks support the

argument that the exchange rate of physical associations governs the relaxation dynamics of these materials as long as the timescale of exchange is faster than that of other competing processes (*e.g.*, polymer diffusion). Nonetheless, elucidating the quantitative interconnection between the lifetime of the physical associations and the bulk viscoelastic properties of polymer networks still remains a challenge.[26] The lack of accurate quantitative prediction partially results from the approximation of the exchange rate of physical associations to the dissociation rate of small molecule complexes in dilute solution, a gross oversimplification that neglects important energetic and kinetic effects resulting from solvation, chain connectivity, and cooperativity. Groundbreaking investigations on model poly(*N,N*-dimethylacrylamide) functionalized with histidine and crosslinked with Ni^{2+} illustrate differences in the rates of dissociation and exchange of physical associations in polymer networks.[27] This motivates inspection not only of other time-dependent properties known to be coupled to polymer dynamics (*e.g.,* ionic conductivity), but also of the cooperative and synergistic effects that arise on dynamic responses upon changes in network structure.

Ion transport in polymers is influenced by ion-polymer associations (*i.e.,* solvation) that reversibly break and form on timescales coupling conduction to polymer segmental dynamics. This results from excluded volume interactions requiring polymer segments to accommodate space upon ion motion.[28] The coupling between polymer dynamics and ion transport is an essential feature which distinguishes ion conducting polymers from dilute liquid electrolytes. Due to the nucleophilic nature of conventional polymer electrolytes such as poly(ethylene oxide), long-range cation transport must involve dissociative steps that facilitate hoping between neighboring solvating sites, as polymer segmental motion arising from local reorientation enables only short-range motion within limited regions of space. Thus, only cations that form labile bonds with a polymer can have significant contributions to the ionic conductivity. The mechanism of ion

conduction for anions is fundamentally different, as these do not form strong bonds with polymers so their motion depends primarily on local dynamics such as in concentrated liquid electrolytes,[29] or multicomponent inert gases.[30]

Dynamic polymer networks based on kinetically labile metal-ligand coordination serve as model systems to develop a multi-scale picture between ion-polymer associations, ionic conductivity, and polymer mechanics. The nature and concentration of ligand and metal can be tuned in these materials to enable not only spanning a range of physical association energies, but also controlling the concentration of both elastically active strands and ions known to be critical in the bulk mechanical and conducting properties. In particular, polymers based on imidazole and histidine ligands are interesting due to a preexisting understanding of the reactivity[31] and interactions with transition metal ions in chemical and biological systems.[32] Investigations of these materials have primarily focused on quaternized imidazolium[33-39] and histammonium[40-42] ions (*i.e.,* polymerized ionic liquids), yet imidazole and histidine moieties are capable of interacting with alkali, alkaline earth, and transition metal ions thus promoting salt dissociation and influencing the ion conducting and mechanical properties (Figure 1). From a materials chemistry standpoint, these materials constitute macromolecular analogues of chelating ionic liquids, a set of concentrated electrolytes known to solubilize ions such as Zn^{2+} due to metal-ligand coordination.[43]

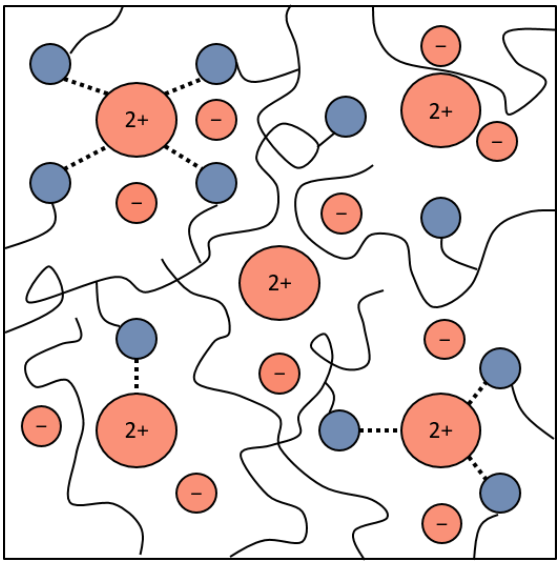

Figure 1. Salt solvation and metal-ligand coordination are coupled due to chemical equilibrium. Based on Le Chatelier's principle, metal-ligand coordination also promotes salt dissociation. This not only translates into a higher concentration of ions, but also on the formation of dynamic crosslinks with important consequences on polymer mechanics. The model system investigated is based on polymers with tethered imidazole ligands, nickel (II) cations (Ni^{2+}), and bis(trifluoromethylsulfonyl)imide anions (NTf_2^-). The number of imidazole moieties coordinating the Ni^{2+} is defined as the coordination number (z). The geometries (z = 1 to 4) are only depicted for illustrative purposes.

We present here, an investigation of the ion conducting and mechanical properties of dynamic polymer networks based on metal-ligand coordination. A combination of ring opening anionic copolymerization, thiol-ene click chemistry, and ligand chemistry is used to rationally design materials for elucidation of structure-property relationships. In particular, we focus on the effect of concentration of nickel (II) bis(trifluoromethylsulfonyl)imide salt on the ion conducting and mechanical properties of a poly(ethylene oxide) with tethered imidazole ligands. Upon physically crosslinking with Ni^{2+}, dynamic polymer networks exhibit an increase in elastic modulus of an order of magnitude, and a maximum in ionic conductivity presumably due to the tradeoff between ion concentration and ion mobility. The demonstrated relationship between mechanics, ion conduction, and metal-ligand coordination illustrates design rules for the development of novel ion conducting polymers. As opposed to composites based on structural insulating agents (*e.g.,* polymer nanocomposites or block copolymers),[44, 45] incorporation of

transition metal ions into polymers with tethered ligand moieties allows for bulk mechanical reinforcement with beneficial effects on ion transport.

Experimental Section

Materials

All materials were used as received from Sigma-Aldrich unless otherwise noted. $CDCl_3$ and methanol-d_4 were purchased from Cambridge Isotope Laboratories; acetonitrile, hexanes, methanol, and isopropyl alcohol from BDH Chemicals; allyl glycidyl ether (AGE) from TCI America; and anhydrous nickel (II) bis(trifluoromethylsulfonylimide) from Alfa Aesar. Tetrahydrofuran (THF) was collected from a commercial J. C. Meyer dry solvent system and used immediately thereafter. AGE was dried over butyl magnesium chloride, degassed through three freeze-pump-thaw cycles, and further distilled to a flame-dried receiving flask. Ethylene oxide (EO) was degassed through three freeze-pump-thaw cycles, and further distilled to a flame-dried buret immersed in an ice bath until use. Potassium naphthalenide was prepared from potassium and naphthalene in THF (0.3 M) and stirred with a glass-coated stir bar for 24 h before use.

Synthesis of N-(2-(1*H*-Imidazol-1-yl)propyl)-4-mercaptobutanamide (Im-SH)

The synthesis of Im-SH was adapted from Lundberg et al.[46] In a 250 mL round-bottom flask equipped with a Teflon™-coated stir bar and a condenser, 1-(3-aminopropyl)imidazole (10.0 g, 79.9 mmol), γ-thiobutyrolactone (8.2 g, 80.2 mmol), and acetonitrile (135 mL) were added. The reaction was heated to 95 ºC and allowed to proceed for 12 h. The reaction was cooled to room temperature, and the resulting pale yellow liquid isolated by evaporation *in vacuo*.

Synthesis of Poly[(ethylene oxide)-*stat*-(allyl glycidyl ether)] (PEO-*stat*-PAGE)

The copolymerization of EO and AGE was adapted from Lee et al.[47] Separate burets containing THF and EO were connected to a thick-walled glass reactor fitted with Ace threads.

The EO was connected by flexible stainless steel bellows so that the buret could be immersed in an ice bath until use. The reactor assembly was flame dried and then cycled between vacuum and positive argon pressure (5 psig) three times. The reactor was finally charged with an argon atmosphere and isolated from the Schlenk line. THF was added, and the temperature equilibrated at 0 ºC. Based on the amount of purified EO (22.77 g, 517 mmol), a quantity of benzyl alcohol (166 μL, 1.60 mmol) was added through a gastight syringe. Potassium naphthalenide (0.3 M in THF) was added through a gastight syringe to titrate the benzyl alcohol until a pale green endpoint. EO was added by lifting the cold buret and allowing monomer to drain in the reactor while AGE (15 mL, 127 mmol) was simultaneously added via gastight syringe. The temperature was increased to 40 ºC, and the polymerization allowed to proceed for 24 h. After complete conversion of EO and AGE, degassed and acidified isopropyl alcohol was added to terminate the polymerization. The resulting PEO-*stat*-PAGE was precipitated into an excess of hexanes, and dried for 48 h at 55 ºC *in vacuo*. PEO-*stat*-PAGE was immediately transferred to a glovebox and stored in an inert nitrogen atmosphere to mitigate moisture uptake.

Synthesis of Imidazole Functionalized Copolymer (PEO-*stat*-PIGE)

In a 250 mL round-bottom flask equipped with a Teflon™-coated stir bar, PEO-*stat*-PAGE (3.00 g, 8.94 mmol of allyl groups), Im-SH (5.08 g, 22.35 mmol), 2,2-dimethoxy-2-phenylacetophenone (DMPA, 0.46 g, 1.79 mmol) and methanol (90 mL) were added. The solution was degassed sparging with nitrogen for 30 min and then allowed to react for 2 h under UV irradiation (λ = 365 nm). The resulting PEO-*stat*-PIGE was concentrated by rotary evaporation, purified by dialysis in methanol (4 times 4 L), and dried for 48 h at 55 ºC *in vacuo* to yield a pale yellow viscoelastic liquid. PEO-*stat*-PIGE was immediately transferred to a glovebox and stored in an inert nitrogen atmosphere to mitigate moisture uptake.

Synthesis of Polymers based on Imidazole-Nickel Coordination (PIGE-Ni^{2+})

In an inert atmosphere, stock solutions in anhydrous methanol of polymer (126 μL, 39.6 wt%, 88 μmol of imidazole) and nickel(II) bis(trifluoromethylsulfonyl)imide were mixed in 5 mL vials to yield materials with an appropriate molar ratio of nickel (II) to imidazole (*i.e.*, r = [Ni^{2+}]:[Im]). The resulting ion conducting dynamic polymer networks were stored in the glovebox to mitigate moisture uptake.

Molecular Characterization

Gel permeation chromatography (GPC) was performed on a Waters instrument using a refractive index detector and Agilent PL gel 5 μm MiniMIX-D column. THF at 35 ºC was used as the mobile phase with a flow rate of 1.0 $mL.min^{-1}$. Polydispersity index (Đ) was determined against PEO narrow standards (Agilent). ^1H NMR spectra were collected on a Bruker Avance DMX 500 MHz. The molecular weight of the precursor PEO-*stat*-PAGE was determined using ^1H NMR end-group analysis (Figure S3). This spectrum is collected in $CDCl_3$ at a polymer concentration of 60 $mg.mL^{-1}$ with 128 scans and a pulse delay time of 5 s.

General Protocol for PIGE-Ni^{2+} Sample Preparation

All polymer samples were kept rigorously dry throughout the described experiments. Polymer samples were prepared in an inert nitrogen atmosphere by casting solutions of PIGE-Ni^{2+} into standard substrates (*e.g.*, aluminum pans, Teflon, and indium tin oxide) and drying *in vacuo* at 55 ºC sequentially for 8 h in the glovebox (10^{-3} torr) and 1 h in a high vacuum oven (10^{-8} torr). Traces of water and methanol in a representative PIGE-Ni^{2+} sample were below detection limits of both Karl-Fischer titration and solid-state ^1H NMR.

Thermal Characterization

Polymer samples were cast as described above into standard aluminum pans. The samples were sealed, and characterized with a Perkin Elmer DSC 8000 to measure the glass transition temperature (T_g) on second heating at 20 $^oC.min^{-1}$ using the onset method.

Mechanical Characterization

The rheology of the samples was characterized using 8 mm stainless steel parallel plates in a TA Instruments ARG2 rheometer operating under dry nitrogen flow. Sample thicknesses were approximately 200 μm. Dynamic frequency sweeps were performed over a range of temperature, frequency, and strain amplitude respectively of 5 °C to 70 ^oC, 0.1 $rad.s^{-1}$ to 100 $rad.s^{-1}$, and 0.1 % to 10 %. Strain sweeps at 10 $rad.s^{-1}$ confirmed that measurements were performed in the linear viscoelastic regime. The reference temperature (T_{ref}) used for time-temperature superposition was either 30 ^oC or T_g and master curves were generated using horizontal shift factors. The elastic modulus was defined as G' at the frequency at which G" exhibits a local minimum (*i.e.*, local maximum in tan(δ)). The terminal relaxation time was determined at the frequency at which the power-law fit of the complex viscosity intersects the zero-shear viscosity.

Electrochemical Impedance Spectroscopy

Polymer samples were prepared as described above by casting into ¼'' clean circular indium tin oxide (ITO) substrates top-coated with a 150 μm Kapton spacer. The samples were sealed with clean ITO substrates and characterized with a Biologic SP-200 potentiostat. Transparent ITO/glass electrodes were used to assure the absence of bubbles and proper interfacial contact during *in situ* conductivity measurements. A sinusoidal voltage with amplitude 100 mV was applied in the frequency range of 1 Hz – 1 MHz. Ionic conductivity, in the absence of concentration gradients, was determined from the real component of the complex conductivity at the peak frequency in tan(δ) arising from the conversion of complex impedance into dielectric

storage and loss.[48] This method is equivalent to determining the ionic conductivity from the impedance at the abscissa intercept of a Nyquist plot. Note that the materials presented herein contain two types of mobile ions: bis(trifluoromethylsulfonyl)imide anions (*i.e.,* NTf_2^-) and Ni^{2+} cations, and the contributions to the current (*i.e.,* transference number) from each of them will depend on the operating conditions of the electrochemical device.[29, 49]

Results and Discussion

1. Molecular Design

Ion transport in dynamic polymer networks based on metal-ligand coordination is anticipated to be intimately coupled to salt dissociation, ion-polymer associations, and polymer segmental dynamics (Figure 1). The incorporation of ligands in a polymer of low dielectric constant promotes salt dissociation to enhance both the ionic conductivity and elastic modulus via formation of labile bonds that serve as dynamic crosslinks. The relatively weak binding energies of these crosslinks enable breakage and formation on timescales that not only hinder polymer diffusion, but also affect ion transport. Although the bulk mechanical and ion conducting properties are influenced by the lifetime of metal-ligand bonds, the underlying molecular mechanisms associated with polymer diffusion and ion transport are different. The former requires the successive breaking of various crosslinks to allow a polymer chain to diffuse;[12, 19, 20] whereas the latter appears to be a more convoluted effect between ion concentration, mobility, and solvation.[28]

To elucidate the relationship between ion conduction, mechanics, and metal-ligand coordination, we engineered a polymer with ligand moieties covalently bonded to the backbone and capable of facilitating salt dissociation by forming dynamic crosslinks. The molecular properties that we sought to control are the nature and concentration of ligand and metal, as these

dictate the lability and lifetime of the crosslinks. This was achieved on a mixture of poly(ethylene oxide) with tethered imidazole moieties and nickel (II) bis(trifluoromethylsulfonyl) imide salt. The complexation between Ni^{2+} and imidazole is anticipated to be the primary interaction dictating the mechanical and ion conducting properties, since the formation of Ni^{2+}-imidazole complexes is thermodynamically favored relative to Ni^{2+}-crown ethers.[32, 50] The weak electrostatic interactions resulting from large and charge-delocalized ions resemble that of chelating ionic liquids, yielding 'plasticized' and amorphous polymers which even at high concentrations exhibit low glass transition temperatures (*i.e.*, T_g). These materials constitute the metal-ligand analogues of proton and hydroxide conducting polymers involving Brønsted acid-base pairs, and are suitable to elucidate structure-property relationships at high ion concentrations due to the thermal processability enabled by sub-ambient T_g.

The synthesis of ion conducting dynamic polymer networks is based on a combination of ionic copolymerization, click chemistry, and metal-ligand interactions (Scheme 1). First, the imidazole functionalized copolymer (*i.e.*, PEO-*stat*-PIGE) was synthesized using epoxide ring opening anionic copolymerization of ethylene oxide (EO) and allyl glycidyl ether (AGE), followed by UV activated thiol-ene click chemistry of N-(2-(1*H*-Imidazol-4-yl)propyl)-4-mercaptobutanamide. PIGE was chosen because the nitrogen atom located in the aromatic ring can coordinate metal ions to facilitate salt dissociation and create dynamic crosslinks. Next, the resulting PEO-*stat*-PIGE was mixed with $Ni(NTf_2)_2$ to generate ion conducting PIGE-Ni^{2+}. Fine and independent control over the ligand and metal nature and concentration can be achieved by replacing the aromatic ring in the thiol or the metal ion, and levering the relative amounts of EO and AGE, and Ni^{2+} and IGE. Here, a series of PIGE-Ni^{2+} with variable molar ratio of Ni^{2+} to IGE (*i.e., r* = $[Ni^{2+}]$:[IGE] = $[Ni^{2+}]$:[Im]) was investigated. Well-defined and narrowly dispersed PEO-

stat-PIGE (M_n = 40 kDa, Đ < 1.2) with a constant mole fraction of imidazole moieties (x_{IGE} = 0.17) was synthesized, as determined using a combination of GPC (Figure S2) and ^{1}H NMR (Figure S3-S4). DSC traces (Figure S5) demonstrate the amorphous nature of the statistical copolymers, a result consistent with the suppression of PEO crystallization in an atactic backbone. The molecular properties and thermal transitions of the various PIGE-Ni^{2+} are summarized in Table 1.

Table 1. Properties of ion conducting dynamic polymer networks based on metal-ligand coordination. [a]Polymers are labeled PIGE-Ni^{2+}X.X, where X.X is the mol% of Ni^{2+} relative to the imidazole ligands. [b,c]Degree of polymerization of EO and IGE in the statistical copolymer determined via ^{1}H NMR end-group analysis. [d]Determined via elemental analysis (Supporting Information). [e]Determined from the molar ratio of Ni^{2+} to imidazole ligands. This ion concentration nomenclature is analogous to that previously reported for Li^+ conducting PEO.[51] [f]Determined via DSC using the onset method.

Polymer[a]	N_{EO}[b]	N_{IGE}[c]	$n_{Ni(NTf2)2}$[d]	r = [Ni^{2+}]:[Im][e]	wt %$_{Ni(NTf2)2}$	T_g (°C)[f]
PIGE-Ni^{2+}0.0	323	79	-	-	-	-33
PIGE-Ni^{2+}3.7	323	79	2.9	0.037	4.2	-31
PIGE-Ni^{2+}12.1	323	79	9.6	0.121	12.6	-29
PIGE-Ni^{2+}14.9	323	79	11.8	0.149	15.1	-23
PIGE-Ni^{2+}16.0	323	79	12.6	0.160	15.9	-12
PIGE-Ni^{2+}19.5	323	79	15.4	0.195	18.8	-2

Scheme 1. Molecular design strategy allows for fine and independent control over the properties expected to have an important effect on metal-ligand coordination, ion conduction, and polymer mechanics: ligand and metal concentration, and identity. This is

respectively achieved by levering the relative amounts of co-monomers in anionic polymerization, the ratio of metal to ligand, the cation in the NTf_2^- salt, and the nucleophilicity of the aromatic ring of the thiol undergoing click chemistry.

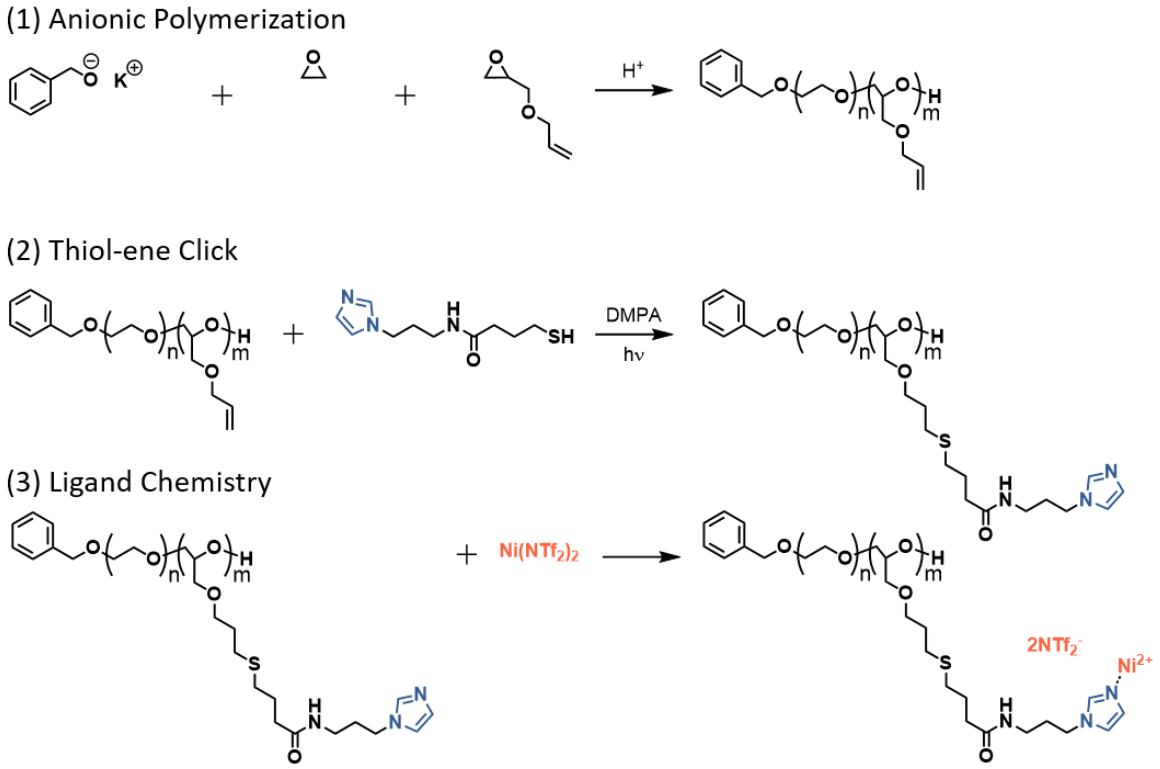

2. Linear Viscoelastic Response

Metal-ligand coordination bonds between Ni^{2+} and imidazole crosslink the PIGE-Ni^{2+} and induce a dramatic change in the bulk mechanical properties. The linear viscoelastic response of these materials is characteristic of associated polymers, with a significant increase in the terminal relaxation time (*i.e.* slower diffusion) and an enhancement in the plateau modulus relative to equivalent polymers without associating groups (Figure 2).[12, 19, 20] Associative polymers exhibit signature features in their dynamic mechanical moduli, including a plateau modulus at high frequencies, a crossover of the storage (G') and loss (G'') moduli, and terminal relaxation with scaling of $G' \sim \omega^2$ and $G'' \sim \omega$. Deviations from this liquid-like scaling observed in PIGE-Ni^{2+} ($G' \sim \omega^{0.9}$ and $G'' \sim \omega^{0.7}$) are attributed to a restricted experimentally accessible low frequency window and hindered polymer diffusion (*i.e.*, sticky reptation). This terminal behavior is

analogous to that of hydrogels based on histidine-functionalized poly(*N,N*-dimethylacrylamide) crosslinked with Ni^{2+}[52] and ionomers based on polyethers and sulfonated phthalates with sodium counterions.[53] The contributions of entanglements to the linear viscoelastic response are neglected due to the absence of a rubbery plateau in neat PIGE. This assertion is further supported by the rheology master curves generated using T_g as the reference temperature (Figure S6) where the mechanical spectra of the polymer melt and associated polymer networks with different *r*-values fail to collapse; an observation consistent with differences in polymer topology and relaxation mechanisms governing the viscoelastic response. At high frequencies the network plateau modulus increases approximately 8-fold from 1.06 MPa to 7.93 MPa for *r*-concentrations respectively of 0.037 and 0.195 (Figure 3b). Moreover, the *G'–G''* crossover frequency ω_c decreases with increasing crosslinker concentration. For example, at 30 °C, ω_c is observed at 21.17 rad.s^{-1} for PIGE-Ni^{2+} with $r = 0.037$ and decreases to 0.19 rad.s^{-1} for $r = 0.257$.

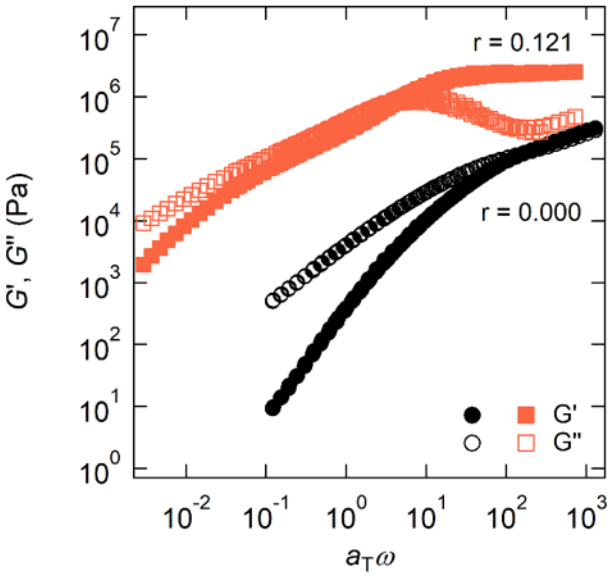

Figure 2. Viscoelastic response of dynamic polymer networks (T_{ref} = 30 °C) arises due to metal-ligand coordination between imidazole moieties tethered to the polymer backbone and Ni^{2+} cations resulting from salt dissociation. Rheology data collected on PIGE-Ni^{2+} under dry N_2 flow.

The effect of Ni^{2+} on the elastic modulus can be explained by changes in polymer topology as a function of ion concentration. In particular, upon increasing the concentration of Ni^{2+} more metal-ligand complexes are formed which initially crosslink PIGE chains while inducing formation of independent network clusters. At a certain critical value of r known as the sol-gel transition (*i.e.*, r_c), a space-spanning percolated network is formed that rapidly becomes more crosslinked with incorporation of additional Ni^{2+}. Here we approximate r_c to be that above which the linear viscoelastic response clearly resembles that of an associating polymer: $r_c \geq 0.121$. Comparisons of r_c with predictions from percolation theory are strictly not possible because the sol-gel transition is not defined for polymer networks with liquid-like terminal relaxation. Nonetheless; assuming PIGE-Ni^{2+} is a chemical network yields $r_c = 0.013$ (Supporting Information). This combination of percolation theory and rheology serves to identify a clear criteria for network formation and is inspired by previous investigations on poly(4-vinylpyridine) crosslinked with *N*,*C*,*N*-pincer Pd (II) complexes.[54]

Enhancements in the elastic modulus above r_c are attributed to an increase in the number of elastically active strands upon addition of Ni^{2+}. Computation of the molar fraction of the various imidazole-Ni^{2+} complexes in chemical equilibrium together with qualitative predictions from sticky-reptation theory support this assertion. Within this framework; only entropy contributes to the free energy, analogous to an ideal gas, and each elastically active strand provides an equal amount of stored energy (*i.e.*, k_BT) to the modulus. Consequently, estimates of the fraction of imidazole-Ni^{2+} complexes that yield elastically active strands provide quantitative insights into the concentration dependence of the modulus. We consider the following chemical equilibria for various Im_nNi^{2+} complexes with n tethered imidazoles coordinating Ni^{2+}:

$$Ni^{2+} + Im \overset{K_1}{\Leftrightarrow} ImNi^{2+}$$

$$ImNi^{2+} + Im \overset{K_2}{\Leftrightarrow} Im_2Ni^{2+}$$

$$Im_2Ni^{2+} + Im \overset{K_3}{\Leftrightarrow} Im_3Ni^{2+}$$

$$Im_3Ni^{2+} + Im \overset{K_4}{\Leftrightarrow} Im_4Ni^{2+}$$

$$Im_4Ni^{2+} + Im \overset{K_5}{\Leftrightarrow} Im_5Ni^{2+}$$

$$Im_5Ni^{2+} + Im \overset{K_6}{\Leftrightarrow} Im_6Ni^{2+}$$

And the corresponding material and charge balances:

$$[Im]_0 = [Im] + [ImNi^{2+}] + 2[Im_2Ni^{2+}] + 3[Im_3Ni^{2+}] + 4[Im_4Ni^{2+}] + 5[Im_5Ni^{2+}] + 6[Im_6Ni^{2+}]$$

$$[Ni^{2+}]_0 = [Ni^{2+}] + [ImNi^{2+}] + [Im_2Ni^{2+}] + [Im_3Ni^{2+}] + [Im_4Ni^{2+}] + [Im_5Ni^{2+}] + [Im_6Ni^{2+}]$$

$$2[NTf_2^-]_0 = [Ni^{2+}]_0$$

For the purposes of this calculation, the equilibrium constants are assumed to be that of small molecule imidazole-Ni^{2+} complexes in aqueous solution of potassium nitrate:[32] $K_1 = 10^{3.03}$ M^{-1}, $K_2 = 10^{2.51}$ M^{-1}, $K_3 = 10^{2.01}$ M^{-1}, $K_4 = 10^{1.47}$, $K_5 = 10^{1.10}$ M^{-1}, and $K_6 = 10^{0.51}$ M^{-1}. Evidently; this simplification neglects differences in physical and chemical environments between aqueous electrolytes and poly(ethylene oxide), yet the resulting equilibrium concentration trends are insensitive to the values of K_n as long as $K_1 \gg K_2 \gg K_3 \gg K_4 \gg K_5 \gg K_6 \gg [Im]_0^{-1}$. The calculated equilibrium mole fractions (Figure 3a) reveal critical features about metal-ligand coordination that influence the bulk mechanical properties such as: (a) the average functionality of the crosslinks at the percolation threshold is six (b) there is a plateau in the concentration of imidazole-Ni^{2+} species (*i.e.*, $x_e = \sum_n n Im_n Ni^{2+}$) that contribute to the formation of elastically active strands at $r \approx 0.160$ (Figure 3b), and (c) at high $Ni(NTf_2)_2$ concentrations there are uncoordinated Ni^{2+} ions ($[Ni^{2+}]$) (Figure 3c). An important underlying assumption behind these assertions is that intramolecular complexation reactions that yield network defects are negligible, an oversimplification that is

rigorously not valid. However, this type of chemical equilibria analysis serves to simply illustrate changes in the distribution of metal-ligand complexes that govern the bulk properties of dynamic polymer networks. Note that although increasing the Ni^{2+} content in the polymer above $r \sim 0.16$ renders a change in coordination geometry, the modulus remains approximately constant due to inconsequential changes in the number of elastically active strands. Consequently, the initial order of magnitude enhancement in modulus upon crosslinking PIGE with Ni^{2+} plateaus upon saturation of imidazole, an observation that demonstrates mechanical stiffening of ion containing polymers via metal-ligand coordination.

Ni^{2+} ions that are not instantaneously coordinated by imidazole ligands or associated with NTf_2^- are solvated by the poly(ethylene oxide) backbone and can play a critical role in preventing bulk polymer flow. Incorporation of solvated Ni^{2+} in the PIGE increases the friction force due to ion-polymer interactions and the terminal relaxation time (Figure 3). This effect is inverse to that previously reported on analogous acrylate copolymers crosslinked with Zn^{2+}, Cu^{2+}, or Co^{2+} where control of the mechanical properties is attained via incorporation of unbound free imidazole ligands.[55] Given that the probability of simultaneous dissociation of all imidazole-Ni^{2+} bonds on a polymer chain is negligible, the terminal relaxation signature for PIGE-Ni^{2+} networks presumably result from the partial and sequential release of the physical associations. PIGE-Ni^{2+} networks with a sufficient ion concentration (*i.e.*, $r > 0.121$) exhibit a terminal relaxation time with a scaling $\tau \sim r^{10.4}$ experimentally obtained from a least-square regression power-law fit. Attempts to compare this observation with theory are not straightforward due to the unknown number of physical associations in polymers based on metal-ligand coordination. This difficulty arises from the microstructure of materials with both ionic groups that can associate into clusters of various sizes and shapes,[56] and metal-ligand complexes that can adopt a range of geometries with distinct

lifetimes.[57] From a theoretical standpoint there are also important limitations, such as the inability to account for stress relaxation mechanisms beyond the formation and breakage of physical associations (*e.g.*, solvation, fluctuations in tube length, and constraint release) in the calculation of the linear viscoelastic response.[58] Nonetheless, the reported increase in terminal relaxation time demonstrates control over the mechanical properties of polymer networks via incorporation of a transition metal ion crosslinker.

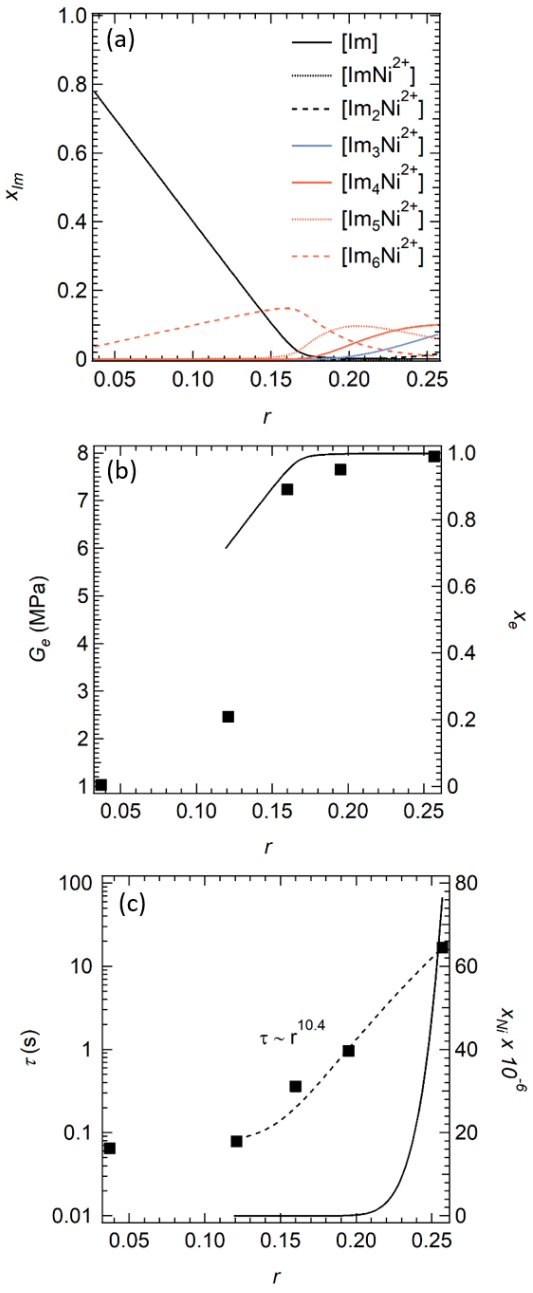

Figure 3. Mechanical properties depend strongly on the molar ratio of Ni^{2+} to imidazole ligands (*r*) **(a)** At the percolation threshold (*i.e.*, $r_c \approx 0.121$) the majority crosslink species is Im_6Ni^{2+} with an average functionality of six. **(b)** The Im_nNi^{2+}crosslinks reinforce the material as revealed by an 8-fold increase in the plateau modulus G_e (■). The plateau modulus was defined as G' at the frequency at which G'' exhibits a local minimum (*i.e.*, local maximum in tan(δ)). Interestingly, the molar fraction of Im_nNi^{2+} species that contribute to the formation of elastically active strands, x_e, (–) and G_e plateau at approximately the same $r \approx 0.160$. This suggests that changes in coordination geometry have a negligible impact in the number of elastically active strands and in the polymer stiffness. **(c)** The terminal relaxation time, τ, (■) increases due to larger friction resulting from ion-polymer interactions between the uncoordinated Ni^{2+} cation (–), poly(ethylene oxide) backbone, and imidazole moieties. The terminal relaxation time was determined at the frequency at which the power-law fit of the complex viscosity (η^*) intersects the plateau zero-shear viscosity (η_0). The scaling experimentally obtained from a least-squares regression power-law fit is $\tau \sim r^{10.4}$.

Overall, the network elasticity and terminal relaxation time are affected by the crosslinker concentration. While the former primarily depends on the instantaneous number density of elastically active strands, the latter results from polymer self-diffusion through a sequence of association and dissociation steps between the ions and the polymer backbone. Polymer self-diffusion is hindered by a combination of solvation and metal-ligand interactions that create a friction force on the polymer chain and increase the terminal relaxation time. Nonetheless, the fast dynamics of solvating interactions prevent the formation of long-term associations capable of contributing to the network elasticity. Thus, polymer stiffness is solely dictated by metal-ligand coordination. This physical picture is qualitatively consistent with sticky-reptation dynamics of associating polymer networks. More quantitative comparisons between theory and experiment are outside the scope of this investigation and only considered in the Supporting Information.

3. Linear Dielectric Response

The incorporation of Ni^{2+} and NTF_2^- ions in PIGE generates a change in the bulk ion conducting properties. The linear dielectric response of these materials is characteristic of ion conducting polymers with a notable enhancement in the ionic conductivity relative to equivalent polymers without ions (Figure 4). The frequency-dependent conductivity exhibits a plateau ionic conductivity at high frequencies (σ_{dc}), a crossover in the real (σ') and imaginary (σ'') conductivity, and terminal relaxation associated with electrode polarization. Note that an important fraction of the electric dipoles are directly associated with the incorporated Ni^{2+} and NTf_2^- ions, but some result from either impurities or uneven electron density distributions in covalent bonds between carbon and heteroatoms. Thus, the presence of a σ_{dc} in neat PIGE is attributed to ionic impurities residual from the polymer synthesis (*e.g.*, potassium naphthalenide). The effect on σ_{dc} upon incorporation of $Ni(NTf_2)_2$ demonstrates that mechanical reinforcement of polymers via metal-

ligand coordination also has important consequences on functional material properties such as the ionic conductivity.

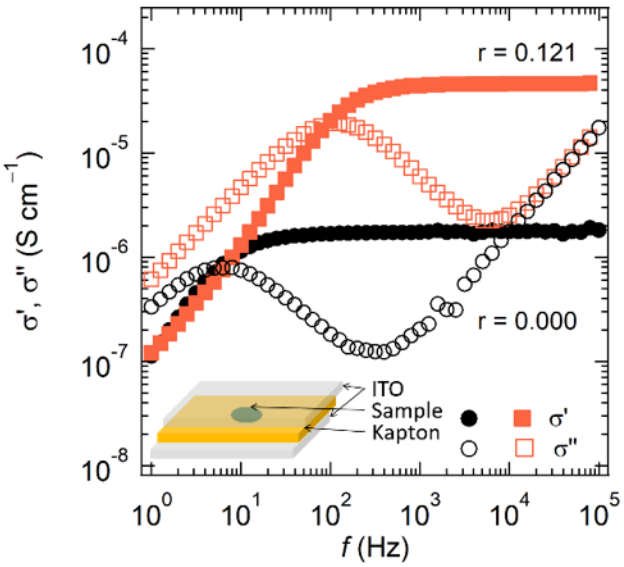

Figure 4. Dielectric response of dynamic polymer networks changes upon incorporation of $Ni(NTf_2)$ due to salt dissociation. Real (σ') and imaginary (σ'') part of the complex conductivity as a function of frequency. The direct current conductivity (σ_{dc}) was defined as σ' at the frequency at which σ'' exhibits a local minimum (*i.e.*, local maximum in tan(δ)). The inset shows a schematic of the *in situ* conductivity measurement cell comprised of the polymer in between two ITO/glass transparent electrodes, separated by 150 μm Kapton spacer.

The maximum in ionic conductivity as a function of salt content reveals the tradeoff between increasing ion concentration and decreasing ion mobility (Figure 5a). Upon incorporation of $Ni(NTf_2)$; there is an enhancement in salt dissociation and an increase in the concentration of ions due to Le Chatelier's principle of chemical equilibrium. However, the formation of metal-ligand complexes also imposes restrictions on polymer segmental dynamics as measured by an increase in T_g (Table 1); a change detrimental for the ion mobility because polymers need to accommodate space upon ion motion. Thus, upon normalization by T_g (*i.e.* comparison with a fixed difference in temperature and T_g, as measured by calorimetry) there is a monotonic increase in the ionic conductivity with ion concentration (Figure 5b). This observation is consistent with that reported for chemically crosslinked ion-conducting networks generated from copolymerization of ionic liquid monomers with varying contents of multi-functional

crosslinkers,[59] and polymer electrolytes based on PEO and $LiNTf_2$.[51] Although the complexation of Ni^{2+} by imidazole moieties couples ion transport to the polymer segmental dynamics, this does not translate into a single NTf_2^- conductor, such as polymerized ionic liquids based on imidazolium,[33-39] as the kinetically labile nature of metal-ligand coordination bonds allows for bond breakage and formation on time scales that could facilitate long-range Ni^{2+} transport as long as the operating temperature is above T_g. A more quantitative relationship between ion content and mobility is currently under investigation and outside the scope of this work. Nonetheless, the presented results demonstrate a competition between ion concentration and bulk (*i.e.*, continuum) ion mobility. A more detailed discussion on the effect of structural heterogeneities, presumably resulting from the incorporation of $Ni(NTf_2)_2$ on a PIGE of low dielectric constant, on the ionic mobility is included in the Supporting Information.

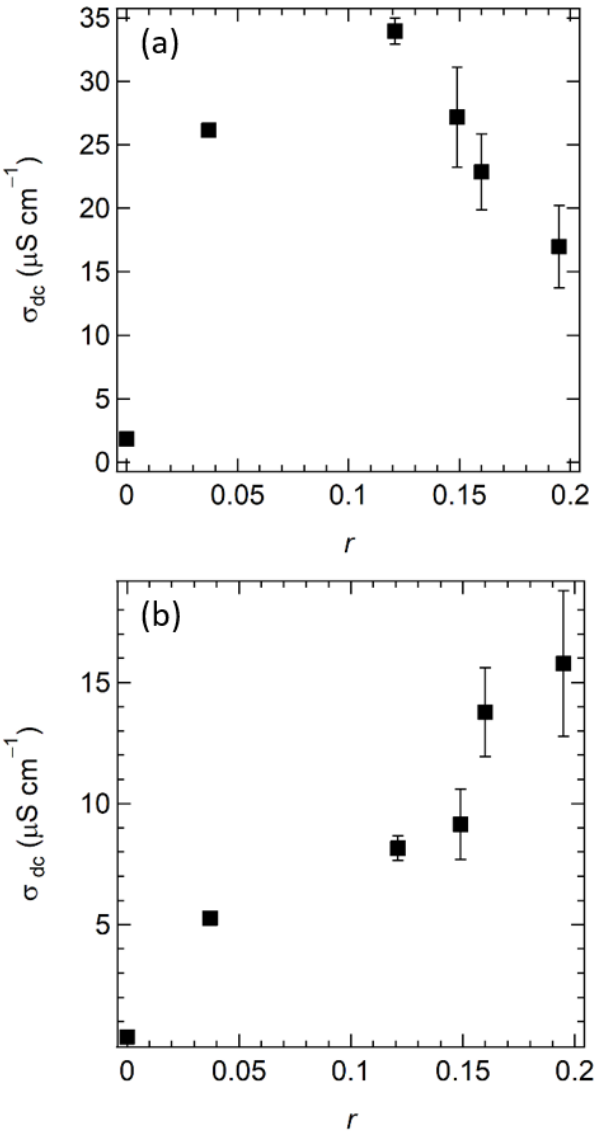

Figure 5. The ionic conductivity as a function of Ni^{2+} concentration. **(a)** Ion conducting dynamic polymer networks based on metal-ligand coordination exhibit a maximum in ionic conductivity due to a competition between ion concentration and ion mobility. Data collected at 90 °C in an inert N_2 atmosphere. Error bars represent 95% confidence intervals and when not depicted are smaller than the symbol ■. **(b)** Monotonic increase in the ionic conductivity due to normalization by the glass transition temperature ($T-T_g$ = 90 °C). Error bars represent 95% confidence intervals and when not depicted are smaller than symbol ■.

The change in polymer segmental dynamics due to formation of dynamic crosslinks has an influential but not determinant effect on the ionic conductivity. The different temperature dependence of the bulk ionic conductivity and fluidity (*i.e.*, inverse of the zero-shear viscosity) for the series of PIGE+Ni^{2+} indicates a partial disconnect between ion and polymer segmental motion, as completely coupled dynamic properties are governed by the same shift factors and exhibit

microscopic relaxation times with identical temperature dependences. Upon Williams-Landel-Ferry normalization (T_{ref} = 30 °C), the C_1 parameter is 30–70 % lower for bulk ion conduction than for polymer flow (Figure 6), with a statistically significant maximum at a *r*-concentration of 0.121. Assuming that the primary impediment to molecular motion is entropic in nature (*i.e.*, there is space available to move) rather than energetic (*i.e.*, there is thermal energy to overcome an activation barrier), this observation suggests (i) that the fractional free volume available for motion is 30–40 % larger for ions than for polymers and (ii) the maximum in ionic conductivity corresponds to the salt concentration at which there is a larger difference in fractional free volume for ion conduction and polymer flow. Although there is disagreement as to which of several different data analysis gives the best value for the free volume, the aforementioned observation qualitatively suggests that ion transport and polymer self-diffusion are molecularly governed by processes with distinct relaxation times. The rigorous assessment of the extent of coupling between ion transport and polymer segmental dynamics requires evaluation of the ratio between the relaxation times,[62] yet the high frequency upturn in the real part of the conductivity is experimentally inaccessible (Figure 4). Further work is necessary not only to quantify the extent of coupling between ion and structural dynamics, but also to elucidate the molecular mechanisms of ion transport (*i.e.*, hopping and molecular diffusion) that contribute to the conductivity and account for the observed differences in fractional free volume. Nonetheless, the illustrated discrepancy in the temperature dependence of the shift factors combined with a monotonic increase in the ionic conductivity upon normalization by T_g (Figure 5b) reasserts the tradeoff between ion concentration and ion mobility which is critical to understand the relationship between metal-ligand coordination and bulk material properties.

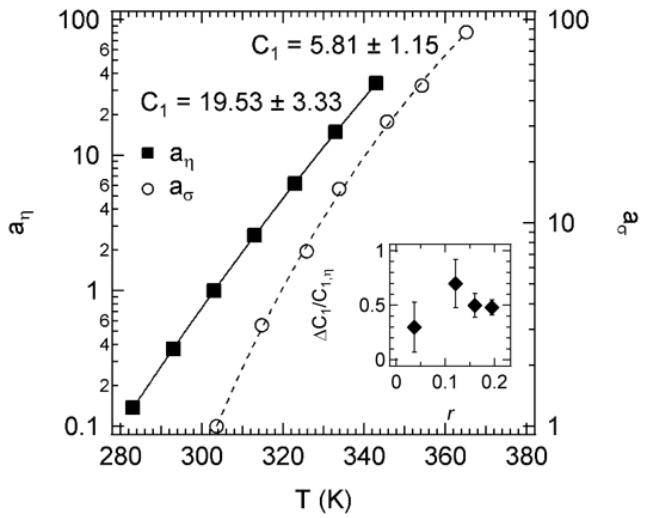

Figure 6. The temperature dependence of the shift factors for the ionic conductivity (○) and fluidity (■) of a representative dynamic polymer network based on metal-ligand coordination (r = 0.121) demonstrates incomplete coupling between ion and polymer segmental motion. The C_1 parameters obtained from a least-squares regression Williams-Landel-Ferry fit for the shift factors of the ionic conductivity and fluidity are respectively 5.81 ± 1.15 and 19.53 ± 3.33. The reference temperature was 30 °C.

Conclusions

The incorporation of transition metal ions into polymers with tethered ligand moieties constitutes a design strategy for mechanically reinforcing polymers with beneficial effects for ion transport, as opposed to the detriments arising from structural but insulating domains intrinsic to polymer nanocomposites[45] or block copolymers.[44] The presented molecular design for ion conducting dynamic polymer networks allows for independent control over the nature and concentration of metal and ligand, and thus can be exploited to elucidate the interconnection between metal-ligand coordination, mechanics, and ion conduction. The formation of dynamic crosslinks upon incorporation of transition metal ions in polymers with tethered ligand moieties increases the number of elastically active strands, and enhances the plateau modulus by an order of magnitude. However, the associated restrictions in polymer segmental dynamics and ion mobility are detrimental for ion transport and yield a maximum in ionic conductivity. The different temperature dependence of the fluidity and ionic conductivity suggests that more fractional free volume is required for ion conduction than for polymer diffusion, yet further work is necessary to

unravel the detailed mechanisms of ion and polymer motion that account for this observation. Nonetheless, the demonstrated structure-property relationship illustrates a rational design rule for novel functional polymers with applications ranging from energy storage and conversion, to medicine.

Supporting Information.

The following files are available free of charge: ^{1}H NMR, GPC, DSC, and rheology master curves referenced to the glass transition temperature. The SI also contains calculation of M_n using ^{1}H NMR end-group analysis, determination of Ni^{2+} content via elemental analysis, discussion of the applicability of percolation theory to PIGE-Ni^{2+}, predictions of elasticity at high *r*-concentrations, comparisons of the modulus with sticky reptation theory, material design rules based on dilute electrolyte theory, and consideration of the role of ionic associations on the ionic mobility.

Corresponding Author

*R.A.S (segalman@ucsb.edu)

Present Addresses

†Sciences et Ingénierie de la Matière Molle, CNRS UMR 7615, École Supérieure de Physique et de Chimie Industrielles de la Ville de Paris (ESPCI), ParisTech, PSL Research University, 10 Rue Vauquelin, F-75231, Paris Cedex 05, France.

§Department of Materials Science and Engineering, University of Illinois, Urbana, Illinois, 61801, United States.

Author Contributions

C.M.E and R.A.S conceived the idea of ion transport in polymers based on metal-ligand coordination. G.E.S and R.A.S designed the polymer to have a low glass transition temperature; and control ligand and metal concentration, and identity. G.E.S, N.S.S and J.M.B acquired, analyzed, and interpreted the data. R.S, M.E.H, and R.A.S critically revised the manuscript. The manuscript was written through contributions of all authors. All authors have given approval to the final version of the manuscript. ‡These authors contributed equally.

Notes

The authors declare no financial interest.

Acknowledgement

This work was supported by the MRSEC Program of the National Science Foundation under Award No. DMR 1720256. G.E.S gratefully acknowledges the AFOSR MURI program under FA9550-12-1, and the UARC ICB program under W911NF-0001 for financial support. N.S.S acknowledges the Fannie and John Hertz Foundation, the Holbrook Foundation Fellowship through the UCSB Institute for Energy Efficiency, and the National Science Foundation Graduate Research Fellowship Program under Grant No. 1650114. Any opinions, findings, and conclusions or recommendations expressed in this material are those of the author(s) and do not necessarily reflect the views of the National Science Foundation. The authors also thank Prof. Costantino Creton, Prof. Lynn M. Walker and Dr. Shubhaditya Majumdar for helpful discussions, and Rogelio Chovet for support in Figure design.

References

1. Cordier, P.; Tournilhac, F.; Soulie-Ziakovic, C.; Leibler, L. Self-Healing and Thermoreversible Rubber from Supramolecular Assembly. *Nature.* **2008,** 451 (7181), 977-980.

2. Guo, M.; Pitet, L. M.; Wyss, H. M.; Vos, M.; Dankers, P. Y. W.; Meijer, E. W. Tough Stimuli-Responsive Supramolecular Hydrogels with Hydrogen-Bonding Network Junctions. *J. Am. Chem. Soc.* **2014,** 136 (19), 6969-6977.
3. Hunt, J. N.; Feldman, K. E.; Lynd, N. A.; Deek, J.; Campos, L. M.; Spruell, J. M.; Hernandez, B. M.; Kramer, E. J.; Hawker, C. J. Tunable, high modulus hydrogels driven by ionic coacervation. *Adv. Mater.* **2011,** 23 (20), 2327-31.
4. Lemmers, M.; Sprakel, J.; Voets, I. K.; van der Gucht, J.; Cohen Stuart, M. A. Multiresponsive reversible gels based on charge-driven assembly. *Angew. Chem. Int. Ed.* **2010,** 49 (4), 708-11.
5. Holten-Andersen, N.; Harrington, M. J.; Birkedal, H.; Lee, B. P.; Messersmith, P. B.; Lee, K. Y.; Waite, J. H. pH-induced metal-ligand cross-links inspired by mussel yield self-healing polymer networks with near-covalent elastic moduli. *Proc. Natl. Acad. Sci.* **2011,** 108 (7), 2651-5.
6. Yount, W. C.; Loveless, D. M.; Craig, S. L. Strong Means Slow: Dynamic Contributions to the Bulk Mechanical Properties of Supramolecular Networks. *Angew. Chem. Int. Ed.* **2005,** 44 (18), 2746-2748.
7. Appel, E. A.; Biedermann, F.; Rauwald, U.; Jones, S. T.; Zayed, J. M.; Scherman, O. A. Supramolecular Cross-Linked Networks via Host−Guest Complexation with Cucurbit[8]uril. *J. Am. Chem. Soc.* **2010,** 132 (40), 14251-14260.
8. Harada, A.; Kobayashi, R.; Takashima, Y.; Hashidzume, A.; Yamaguchi, H. Macroscopic Self-Assembly through Molecular Recognition. *Nat. Chem.* **2011,** 3 (1), 34-37.
9. Alexandridis, P.; Holzwarth, J. F.; Hatton, T. A. Micellization of Poly(ethylene oxide)-Poly(propylene oxide)-Poly(ethylene oxide) Triblock Copolymers in Aqueous Solutions: Thermodynamics of Copolymer Association. *Macromolecules.* **1994,** 27 (9), 2414-2425.
10. Petka, W. A.; Harden, J. L.; McGrath, K. P.; Wirtz, D.; Tirrell, D. A. Reversible Hydrogels from Self-Assembling Artificial Proteins. *Science.* **1998,** 281 (5375), 389.
11. Green, M. S.; Tobolsky, A. V. A New Approach to the Theory of Relaxing Polymeric Media. *J. Chem. Phys.* **1946,** 14 (2), 80-92.
12. Tanaka, F.; Edwards, S. F. Viscoelastic Properties of Physically Crosslinked Networks. 1. Transient Network Theory. *Macromolecules.* **1992,** 25 (5), 1516-1523.
13. Wang, C.; Wu, H.; Chen, Z.; McDowell, M. T.; Cui, Y.; Bao, Z. Self-Healing Chemistry Enables the Stable Operation of Silicon Microparticle Anodes for High-Energy Lithium-Ion Batteries. *Nat. Chem.* **2013,** 5 (12), 1042-1048.
14. Stadler, R., Transient networks by hydrogen bond interactions in polybutadiene-melts. In *Permanent and Transient Networks*, Steinkopff: Darmstadt, 1987; pp 140-145.
15. Langer, R.; Tirrell, D. A. Designing Materials for Biology and Medicine. *Nature.* **2004,** 428 (6982), 487-492.
16. Williams, K. A.; Dreyer, D. R.; Bielawski, C. W. The Underlying Chemistry of Self-Healing Materials. *MRS Bull.* **2011,** 33 (8), 759-765.
17. Sun, J.-Y.; Zhao, X.; Illeperuma, W. R. K.; Chaudhuri, O.; Oh, K. H.; Mooney, D. J.; Vlassak, J. J.; Suo, Z. Highly Stretchable and Tough Hydrogels. *Nature.* **2012,** 489, 133-136.
18. Creton, C. 50th Anniversary Perspective: Networks and Gels: Soft but Dynamic and Tough. *Macromolecules.* **2017,** 50 (21), 8297-8316.
19. Leibler, L.; Rubinstein, M.; Colby, R. H. Dynamics of Reversible Networks. *Macromolecules.* **1991,** 24 (16), 4701-4707.

20. Rubinstein, M.; Semenov, A. N. Dynamics of Entangled Solutions of Associating Polymers. *Macromolecules.* **2001,** 34 (4), 1058-1068.
21. Yount, W. C.; Loveless, D. M.; Craig, S. L. Small-Molecule Dynamics and Mechanisms Underlying the Macroscopic Mechanical Properties of Coordinatively Cross-Linked Polymer Networks. *J. Am. Chem. Soc.* **2005,** 127 (41), 14488-14496.
22. Shen, W.; Kornfield, J. A.; Tirrell, D. A. Dynamic Properties of Artificial Protein Hydrogels Assembled through Aggregation of Leucine Zipper Peptide Domains. *Macromolecules.* **2007,** 40 (3), 689-692.
23. Fullenkamp, D. E.; He, L.; Barrett, D. G.; Burghardt, W. R.; Messersmith, P. B. Mussel-Inspired Histidine-Based Transient Network Metal Coordination Hydrogels. *Macromolecules.* **2013,** 46 (3), 1167-1174.
24. Grindy, S. C.; Lenz, M.; Holten-Andersen, N. Engineering Elasticity and Relaxation Time in Metal-Coordinate Cross-Linked Hydrogels. *Macromolecules.* **2016,** 49 (21), 8306-8312.
25. McKinnon, D. D.; Domaille, D. W.; Cha, J. N.; Anseth, K. S. Bis-Aliphatic Hydrazone-Linked Hydrogels Form Most Rapidly at Physiological pH: Identifying the Origin of Hydrogel Properties with Small Molecule Kinetic Studies. *Chem. Mater.* **2014,** 26 (7), 2382-2387.
26. Wang, R.; Sing, M. K.; Avery, R. K.; Souza, B. S.; Kim, M.; Olsen, B. D. Classical Challenges in the Physical Chemistry of Polymer Networks and the Design of New Materials. *Acc. Chem. Res.* **2016,** 49 (12), 2786-2795.
27. Tang, S.; Olsen, B. D. Relaxation Processes in Supramolecular Metallogels Based on Histidine–Nickel Coordination Bonds. *Macromolecules.* **2016,** 49 (23), 9163-9175.
28. Miller, T. F.; Wang, Z. G.; Coates, G. W.; Balsara, N. P. Designing Polymer Electrolytes for Safe and High Capacity Rechargeable Lithium Batteries. *Acc. Chem. Res.* **2017,** 50 (3), 590-593.
29. Newman, J.; Thomas-Alyea, K. E., *Electrochemical Systems*. 3rd ed.; John Wiley & Sons, Inc.: Hoboken, NJ, 2004.
30. Deen, W. M., *Analysis of Transport Phenomena*. 2nd ed.; Oxford University Press: 2012.
31. Letter, J. E.; Jordan, R. B. Kinetic study of the complexing of nickel(II) by imidazole, histidine, and histidine methyl ester. *Inorg. Chem.* **1971,** 10 (12), 2692-2696.
32. Sundberg, R. J.; Martin, R. B. Interactions of Histidine and Other Imidazole Derivatives with Transition Metal Ions in Chemical and Biological Systems. *Chem. Rev.* **1974,** 74 (4), 471-517.
33. Ohno, H.; Ito, K. Room-Temperature Molten Salt Polymers as a Matrix for Fast Ion Conduction. *Chem. Lett.* **1998,** 27 (8), 751-752.
34. Salas de la Cruz, D.; Green, M. D.; Ye, Y.; Elabd, Y. A.; Long, T. E.; Winey, K. I. Correlating backbone-to-backbone distance to ionic conductivity in amorphous polymerized ionic liquids. *J. Polym. Sci. B.* **2012,** 50 (5), 338-346.
35. Choi, U. H.; Ye, Y.; Salas de la Cruz, D.; Liu, W.; Winey, K. I.; Elabd, Y. A.; Runt, J.; Colby, R. H. Dielectric and Viscoelastic Responses of Imidazolium-Based Ionomers with Different Counterions and Side Chain Lengths. *Macromolecules.* **2014,** 47 (2), 777-790.
36. Sangoro, J. R.; Iacob, C.; Agapov, A. L.; Wang, Y.; Berdzinski, S.; Rexhausen, H.; Strehmel, V.; Friedrich, C.; Sokolov, A. P.; Kremer, F. Decoupling of ionic conductivity from structural dynamics in polymerized ionic liquids. *Soft Matter.* **2014,** 10 (20), 3536-3540.
37. Wojnarowska, Z.; Knapik, J.; Díaz, M.; Ortiz, A.; Ortiz, I.; Paluch, M. Conductivity Mechanism in Polymerized Imidazolium-Based Protic Ionic Liquid [HSO3–BVIm][OTf]: Dielectric Relaxation Studies. *Macromolecules.* **2014,** 47 (12), 4056-4065.

38. Evans, C. M.; Bridges, C. R.; Sanoja, G. E.; Bartels, J.; Segalman, R. A. Role of Tethered Ion Placement on Polymerized Ionic Liquid Structure and Conductivity: Pendant versus Backbone Charge Placement. *ACS Macro Lett.* **2016,** 5 (8), 925-930.
39. Bartels, J.; Sanoja, G. E.; Evans, C. M.; Segalman, R. A.; Helgeson, M. E. Decoupling Mechanical and Conductive Dynamics of Polymeric Ionic Liquids via a Trivalent Anion Additive. *Macromolecules.* **2017,** 50 (22), 8979-8987.
40. Evans, C. M.; Sanoja, G. E.; Popere, B. C.; Segalman, R. A. Anhydrous Proton Transport in Polymerized Ionic Liquid Block Copolymers: Roles of Block Length, Ionic Content, and Confinement. *Macromolecules.* **2016,** 49 (1), 395-404.
41. Sanoja, G. E.; Popere, B. C.; Beckingham, B. S.; Evans, C. M.; Lynd, N. A.; Segalman, R. A. Structure–Conductivity Relationships of Block Copolymer Membranes Based on Hydrated Protic Polymerized Ionic Liquids: Effect of Domain Spacing. *Macromolecules.* **2016,** 49 (6), 2216-2223.
42. Schneider, Y.; Modestino, M. A.; McCulloch, B. L.; Hoarfrost, M. L.; Hess, R. W.; Segalman, R. A. Ionic Conduction in Nanostructured Membranes Based on Polymerized Protic Ionic Liquids. *Macromolecules.* **2013,** 46 (4), 1543-1548.
43. Kar, M.; Winther-Jensen, B.; Forsyth, M.; MacFarlane, D. R. Chelating Ionic Liquids for Reversible Zinc Electrochemistry. *Phys. Chem. Chem. Phys.* **2013,** 15 (19), 7191-7197.
44. Bates, C. M.; Bates, F. S. 50th Anniversary Perspective: Block Polymers—Pure Potential. *Macromolecules.* **2017,** 50 (1), 3-22.
45. Kumar, S. K.; Benicewicz, B. C.; Vaia, R. A.; Winey, K. I. 50th Anniversary Perspective: Are Polymer Nanocomposites Practical for Applications? *Macromolecules.* **2017,** 50 (3), 714-731.
46. Lundberg, P.; Lynd, N. A.; Zhang, Y.; Zeng, X.; Krogstad, D. V.; Paffen, T.; Malkoch, M.; Nystrom, A. M.; Hawker, C. J. pH-triggered self-assembly of biocompatible histamine-functionalized triblock copolymers. *Soft Matter.* **2013,** 9 (1), 82-89.
47. Lee, B. F.; Wolffs, M.; Delaney, K. T.; Sprafke, J. K.; Leibfarth, F. A.; Hawker, C. J.; Lynd, N. A. Reactivity Ratios and Mechanistic Insight for Anionic Ring-Opening Copolymerization of Epoxides. *Macromolecules.* **2012,** 45 (9), 3722-3731.
48. Runt, J. P.; Fitzgerald, J. J., *Dielectric Spectroscopy of Polymeric Materials: Fundamentals and Applications*. American Chemical Society: 1997.
49. Balsara, N. P.; Newman, J. Relationship between Steady-State Current in Symmetric Cells and Transference Number of Electrolytes Comprising Univalent and Multivalent Ions. *J. Electrochem. Soc.* **2015,** 162 (14), A2720-A2722.
50. Chen, L.; Bos, M.; Grootenhuis, P. D. J.; Christenhusz, A.; Hoogendam, E.; Reinhoudt, D. N.; Van Der Linden, W. E. Stability Constants for some Divalent Metal Ion/Crown Ether Complexes in Methanol determined by Polarography and Conductometry. *Anal. Chim. Acta.* **1987,** 201, 117-125.
51. Panday, A.; Mullin, S.; Gomez, E. D.; Wanakule, N.; Chen, V. L.; Hexemer, A.; Pople, J.; Balsara, N. P. Effect of Molecular Weight and Salt Concentration on Conductivity of Block Copolymer Electrolytes. *Macromolecules.* **2009,** 42 (13), 4632-4637.
52. Tang, S.; Wang, M.; Olsen, B. D. Anomalous Self-Diffusion and Sticky Rouse Dynamics in Associative Protein Hydrogels. *J. Am. Chem. Soc.* **2015,** 137 (11), 3946-3957.
53. Chen, Q.; Tudryn, G. J.; Colby, R. H. Ionomer dynamics and the sticky Rouse model. *J. Rheol.* **2013,** 57 (5), 1441-1462.
54. Xu, D.; Craig, S. L. Scaling Laws in Supramolecular Polymer Networks. *Macromolecules.* **2011,** 44 (13), 5465-5472.

55. Mozhdehi, D.; Neal, J. A.; Grindy, S. C.; Cordeau, Y.; Ayala, S.; Holten-Andersen, N.; Guan, Z. Tuning Dynamic Mechanical Response in Metallopolymer Networks through Simultaneous Control of Structural and Temporal Properties of the Networks. *Macromolecules.* **2016,** 49 (17), 6310-6321.
56. Eisenberg, A. Clustering of Ions in Organic Polymers. A Theoretical Approach. *Macromolecules.* **1970,** 3 (2), 147-154.
57. Atkins, P., *Shriver and Atkins' Inorganic Chemistry*. 4th ed.; Oxford University Press: New York, 2006.
58. Doi, M.; Edwards, S. F., *The Theory of Polymer Dynamics*. Clarendon Press: 1988.
59. Washiro, S.; Yoshizawa, M.; Nakajima, H.; Ohno, H. Highly ion conductive flexible films composed of network polymers based on polymerizable ionic liquids. *Polymer.* **2004,** 45 (5), 1577-1582.
60. Cukierman, S. Et tu, Grotthuss! and Other Unfinished Stories. *Biochim. Biophys. Acta, Bioenerg.* **2006,** 1757 (8), 876-885.
61. Hoarfrost, M. L.; Tyagi, M.; Segalman, R. A.; Reimer, J. A. Proton hopping and long-range transport in the protic ionic liquid [Im][TFSI], probed by pulsed-field gradient NMR and quasi-elastic neutron scattering. *J. Phys. Chem. B.* **2012,** 116 (28), 8201-9.
62. Angell, C. A. Dynamic Processes in Ionic Glasses. *Chem. Rev.* **1990,** 90 (3), 523-542.

Ion Transport in Dynamic Polymer Networks based on Metal-Ligand Coordination: Effect of Crosslinker Concentration – Supporting Information

*Gabriel E. Sanoja,[1, 2, ‡] Nicole S. Schauser,[3, ‡] Joshua M. Bartels,[2] Christopher M. Evans,[2] Matthew E. Helgeson,[2] Ram Seshadri,[3] and Rachel A. Segalman[2, 3, *]*

[1]Department of Chemical and Biomolecular Engineering, University of California, Berkeley, California 94720, United States

[2]Department of Chemical Engineering and [3]Materials Department, University of California, Santa Barbara 93106, United States

[‡]These authors contributed equally

[*]Email: segalman@ucsb.edu (R.A.S)

Molecular Characterization

Synthesis of N-(2-1H-Imidazol-1-yl)propyl)-4-mercaptobutanamide (Im-SH)

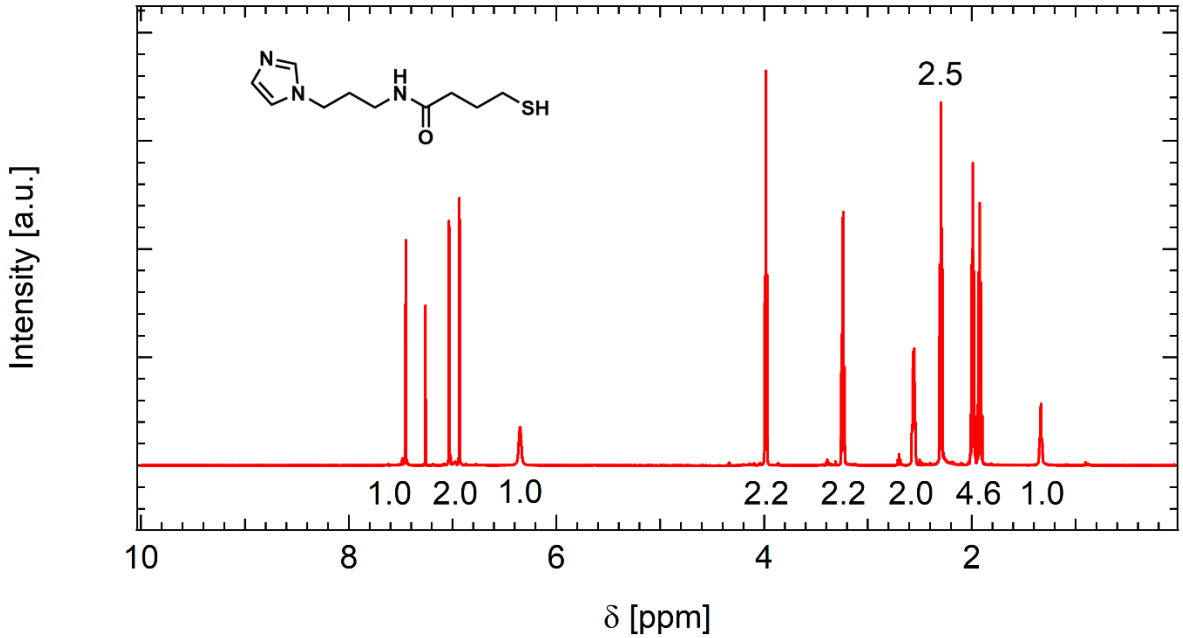

Figure S1: ^{1}H NMR of Im-SH in $CDCl_3$

Synthesis of Poly[(ethylene oxide)-stat-(allyl glycidyl ether)] (PEO-stat-PAGE)

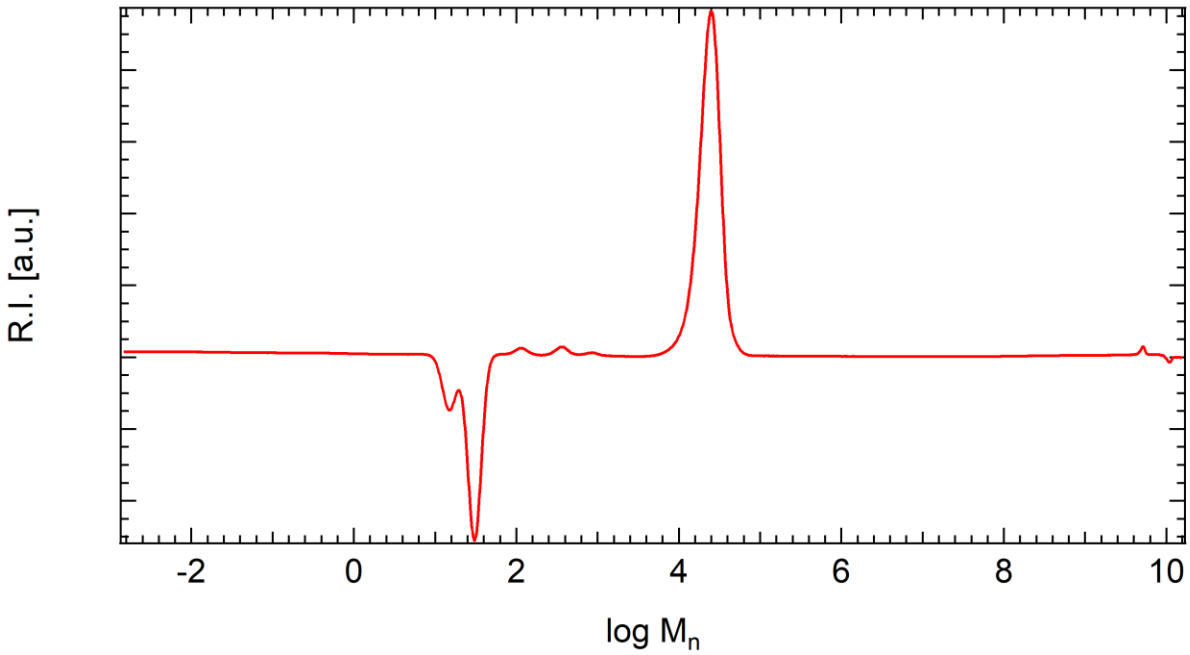

Figure S2: Gel Permeation Chromatography of PEO-*stat*-PAGE calibrated against poly(ethylene oxide) standards. The polydispersity ($Đ = M_n/M_w$) was lower than 1.2. This is consistent with the living nature of the anionic copolymerization of ethylene oxide and allyl glycidyl ether.

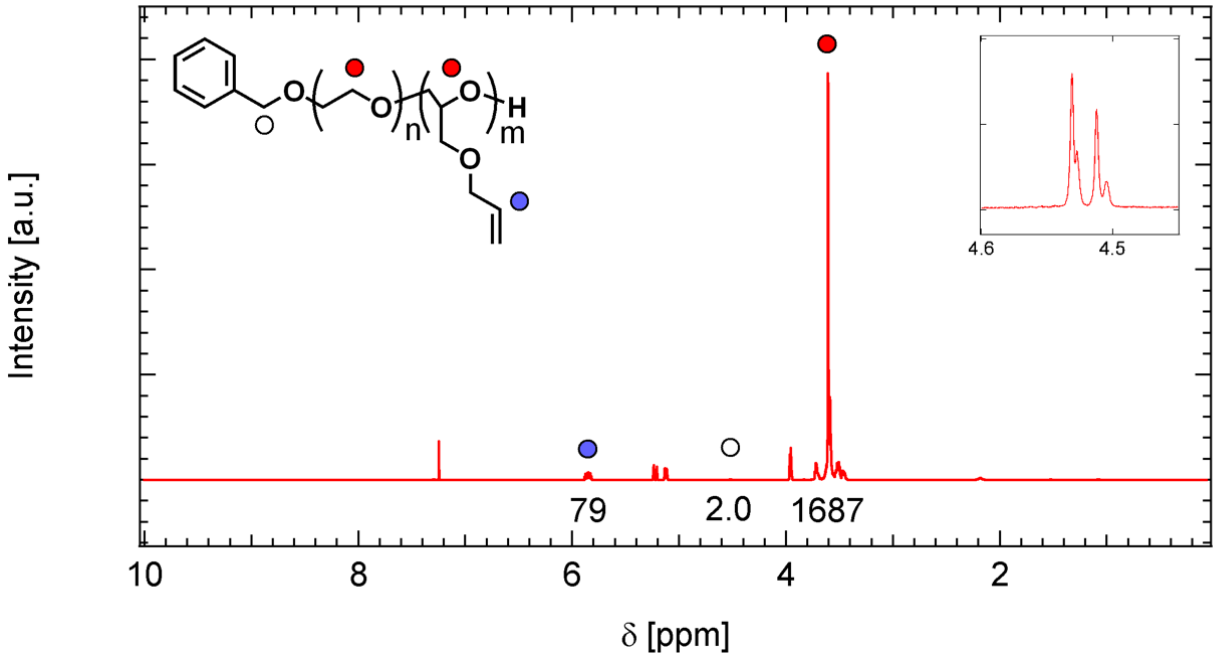

Figure S3: ^{1}H NMR of PEO-*stat*-PAGE in $CDCl_3$. End-group analysis yields the number of repeat units of ethylene oxide and allyl glycidyl ether, PEO_{323}-*stat*-$PAGE_{79}$. Inset illustrates the benzylic hydrogen peaks. This spectrum is collected at a polymer concentration of 60 mg.mL^{-1} with 128 scans and a pulse delay time of 5 s.

From the presented ^{1}H NMR, the number of repeat units in PEO-*stat*-PAGE are given by:

$$m = N_{AGE} = \frac{I_{benzylic}}{2} * I_{allylic} = \frac{2.0}{2} * 79 = 79$$

$$n = N_{EO} = \frac{I_{ether} - (5 * N_{AGE})}{4} = \frac{1687 - (5 * 79)}{4} = 323$$

The resulting polymer is then PEO_{323}-*stat*-$PAGE_{79}$. The end-group peak splitting is attributed to the different reactivity of EO and AGE towards the benzyl alkoxide initiator, a focus of an investigation by Lee et al.[1]

Synthesis of Imidazole Functionalized Copolymer (PEO-stat-PIGE)

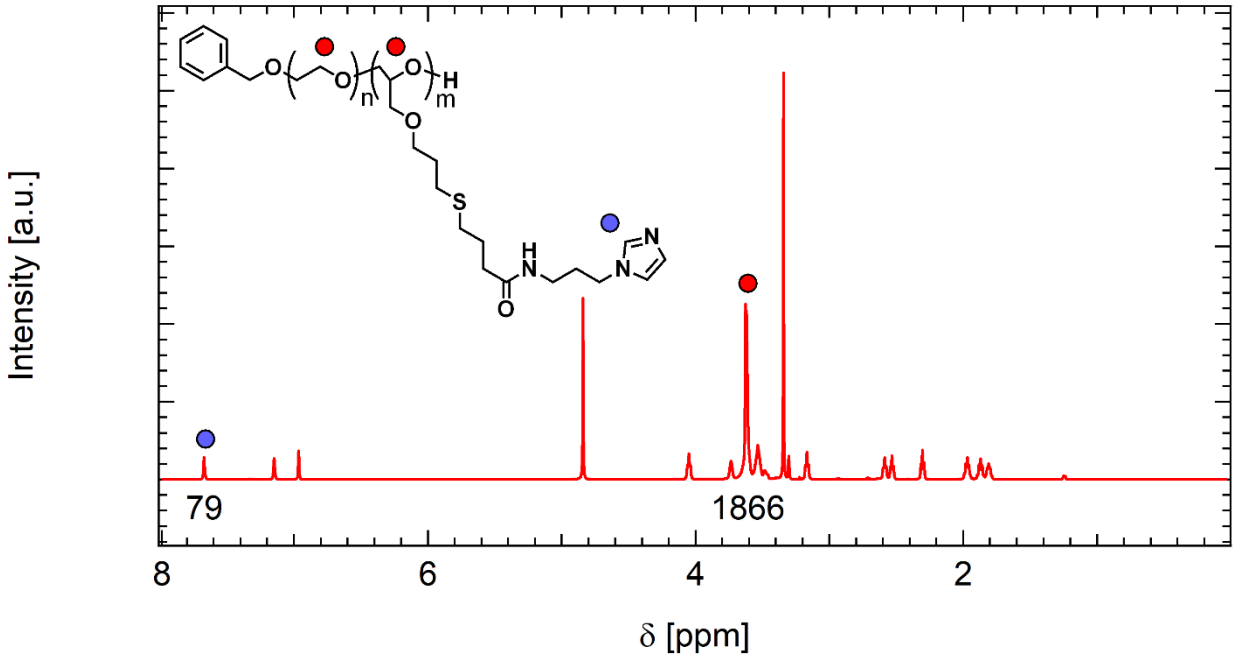

Figure S4: ^{1}H NMR of PEO-*stat*-PIGE in CD_3OD. Disappearance of allyl groups from PEO-*stat*-PAGE and appearance of imidazole aromatic peaks confirm complete conversion during the thiol-ene click reaction.

The presented ^{1}H NMR demonstrates complete conversion of the allylic units into imidazole. The number of repeat units in PEO-*stat*-PIGE are then given by

$$N_{IGE} = \frac{I_{imidazole}}{1} = 79$$

$$N_{EO} = \frac{I_{ether} - (5 * N_{IGE})}{4} = \frac{1866 - (5 * 79)}{4} = 368$$

The resulting polymer is PEO_{79}-*stat*-$PIGE_{368}$, which is consistent with the PEO_{79}-*stat*-$PIGE_{323}$ expected from conservation of moles. For the purposes of this investigation, we use PEO_{79}-*stat*-$PIGE_{323}$ as the ^{1}H NMR end-group analysis requires longer pulse delay times.

Synthesis of Polymers based on Imidazole-Nickel Coordination (PIGE-Ni^{2+})

Table S1. Elemental analysis of ion conducting dynamic polymer networks based on metal-ligand coordination. [a]Polymers are labeled PIGE-Ni^{2+}X.X, where X.X is the mol% of Ni^{2+} relative to the imidazole ligands. [b]Concentration of Ni^{2}. [c]Mass of PIGE-Ni^{2+}X.X polymer. [d]Moles of Ni^{2+} contained in PIGE-Ni^{2+}X.X polymer. [e]Moles of IGE ligand in PIGE-Ni^{2+}X.X polymer. [f]Determined from the molar ratio of Ni^{2+} to imidazole ligands. This ion concentration nomenclature is analogous to that previously reported for Li^{+} conducting PEO.

Polymer[a]	c_{Ni} (ppm)[b]	m (μg)[c]	n_{Ni} (mmol)[d]	n_{IGE} (mmol)[e]	r[f]
PIGE-Ni^{2+}3.7	3660	17.32	1.08	29.3	0.037
PIGE-Ni^{2+}12.1	13200	3.96	0.89	5.99	0.149
PIGE-Ni^{2+}14.9	11000	16.63	3.12	25.8	0.121
PIGE-Ni^{2+}19.5	16600	20.79	5.88	30.1	0.195

Thermal Characterization

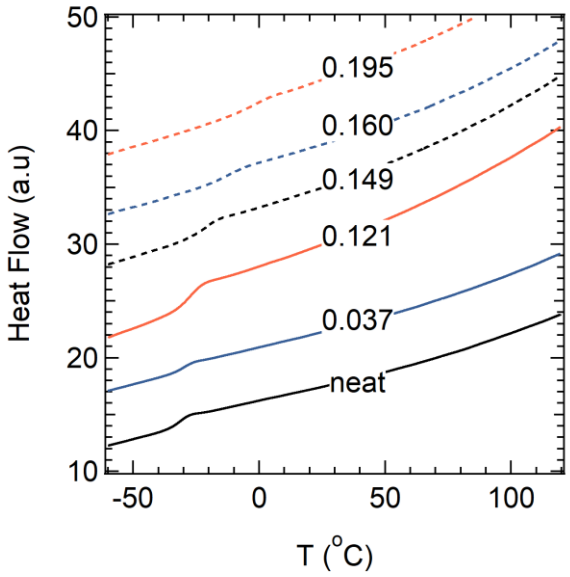

Figure S5. Differential Scanning Calorimetry of PIGE-Ni^{2+} allows for determination of the T_g. Data collected on second heating at 20 $^{o}C.min^{-1}$

The absence of a PEO crystallization/melting peak in the presented DSC traces is consistent with the atactic nature of the PEO-*stat*-PIGE copolymer.

Linear Viscoelastic Response

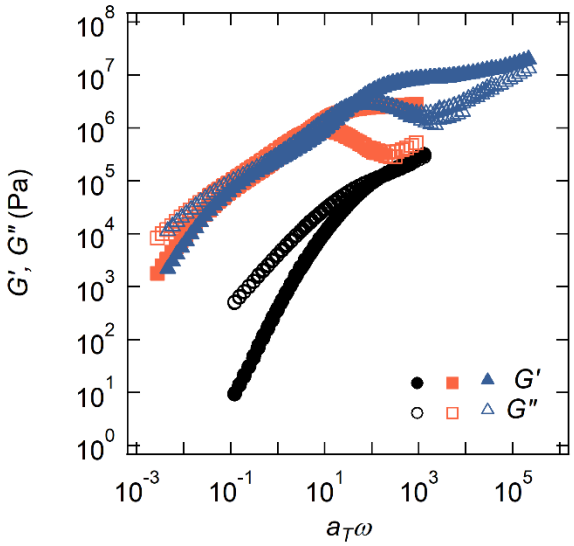

Figure S6. Viscoelastic response of PIGE-Ni^{2+} for *r*-concentration of 0.000 (●, ○) 0.121 (■, □) and 0.195 (▲, Δ) at $T_{ref} = T_g$ arises due to metal-ligand coordination between imidazole moieties tethered to the polymer backbone and Ni^{2+} cations resulting from salt dissociation. Rheology data collected on PIGE-Ni^{2+} under dry N_2 flow.

The contributions of entanglements to the linear viscoelastic response are neglected due to the absence of a rubbery plateau in the neat PIGE. This assertion is further supported by Figure S6, where the mechanical spectra of the polymer melt and associated polymer network fail to collapse at all frequencies; an observation consistent with differences in topology and relaxation mechanisms governing the mechanical properties of these materials.

Percolation Theory and the Sol-Gel Transition

PIGE-Ni^{2+} is a dynamic polymer network where chains are associated via physical interactions. Under a finite stress, the crosslinks eventually split, and the long-time behavior is always liquid-like. Thus, these materials do not have a strict sol-gel transition.

It is still interesting to consider PIGE-Ni^{2+} as chemical networks and evaluate the sol-gel transition using percolation theory. In this case, we start from a dense system of linear chains (degree of polymerization $N = N_{EO} + N_{IGE} \gg 1$) and we crosslink them. This is a similar scenario to the vulcanization of rubber.[2] In this situation, the functionality $z = N_{IGE}$ becomes very large

because each IGE monomer is capable of participating in a crosslink. The sol-gel transition, corresponding to the concentration at which there is one interstrand crosslinker per polymer chain, is then given by $r_c = 1/(N_{IGE} - 1) \cong {N_{IGE}}^{-1} \cong 0.013$. This prediction is below the ion concentration at which there is a stepwise increase in the elastic modulus ($r_c \approx 0.121$), an observation consistent with the existence of topological defects in the infinite cluster. The combinations of this prediction with the linear viscoelastic response of associated polymers serves as a criteria for network formation.

Percolation theory is a mean field theory that generally fails to describe the sol-gel transition of chemically crosslinked networks. The physical picture of this critical phenomenon is based on a "tree approximation", where topological defects such as loops or dangling chains arising from steric hindrances are neglected. This is evidently a gross oversimplification, as excluded volume interactions in a branched molecule are expected to be even stronger than in linear chains.

To understand why the theoretical prediction of the sol-gel transition of PIGE-Ni^{2+} can be considered accurate, it is convenient to follow the formalism elegantly discussed by de Gennes[3] and estimate the number (P) of chains which presumably crosslink directly with one given chain in the melt. The volume spanned by one particular chain C is of order ${R_o}^3 = N^{3/2}a^3$, and the number of chains per unit volume is $1/Na^3$. Any chain C' which has a good overlap with the volume ${R_o}^3$ is certainly in direct contact at some points with C, the number of CC' contacts being of order $N^2a^3/{R_o}^3 \sim N^{1/2}$. Thus, the total number of chains C' probably attached to C is of order $P \cong \frac{1}{Na^3}{R_o}^3 \cong N^{1/2}$. Clearly, $P \gg 1$ ensuring that all deviations from a mean field picture are weak and negligible.

Predictions of Elasticity and Relaxation Time in the Concentration Regime r ≈ 1

A quantitative understanding of the relationship between the physical associations and the linear viscoelastic response is key because the mechanical properties of dynamic polymer networks are not only affected by the crosslinker concentration; but also by the polymer concentration, ligand position, among others. Previous work by Grindy et al. investigated the mechanical properties of model tetra-arm poly(ethylene glycol) hydrogels transiently crosslinked with histidine-Ni^{2+} complexes.[4] While their system is a hydrogel in the semidilute polymer concentration regime that exhibits a maximum in elastic modulus and terminal relaxation time as a function of histidine-Ni^{2+} stoichiometry, these ion concentration dependencies result from changes in the distribution of coordinate complexes, ligands, and free Ni^{2+}. Here we investigate a set of elastomers that exhibit a plateau in elastic modulus and an increasing terminal relaxation time as a function of crosslinker concentration, yet the prediction from the chemical equilibria calculations is that the majority species in the high *r*-concentration regime is elastically inactive $ImNi^{2+}$ and thus the modulus and relaxation times should eventually decrease (Figure S7). Consequently, the presented results do not contradict but instead complement those of Grindy et al., a comparison that again illustrates the importance of the simple, naive, but insightful chemical equilibria analysis considered in both studies.

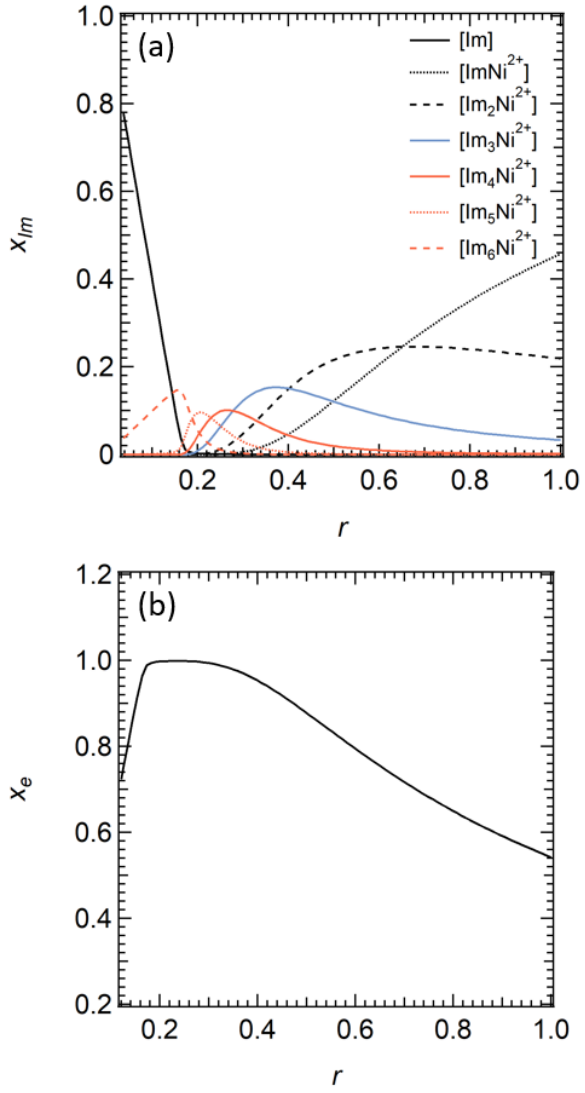

Figure S7. (a) Molar fractions of Im_nNi^{2+} species as estimated from the equilibrium constants K_n. In the concentration regime $r \approx 1.000$, the majority crosslink species is $ImNi^{2+}$ with an average functionality of two. **(b)** The molar fraction of Im_nNi^{2+} species that contribute to the formation of elastically active strands decreases, which should macroscopically translate into a loss of material elasticity.

Comparison between the Elastic Modulus and Sticky Reptation

The elastic modulus (*i.e.*, G_e) experimentally determined for r = 0.195 is 7.7 MPa, a value higher than the 4.4 MPa predicted by the Sticky Reptation model. Although this difference between theory and experiment might appear inconsequential, the Sticky Reptation model unrealistically assumes that every imidazole is associated with a Ni^{2+} ion and that there are no

topological network imperfections. Thus, G_e should be overestimated and careful inspection of the theory is required to reconcile it with experimental observations.

The high value of G_e suggests PIGE-Ni^{2+}19.5 has more network strands than those accounted for by simple macromers (*i.e.*, approximately one IGE per five EO according to the stoichiometric ratio). Thus, we consider the case where both the chain pendants and the EO strands between IGE segments behave as elastically active strands (Figure S8). This is possible since the pendant molecular weight (and presumably the size) is similar to that of the macromer. The result is a higher concentration of network strands with an associated modulus given by the equipartition theorem: $G_e = (\nu_1 + \nu_2)kT$. Here, ν_1 and ν_2 are respectively the density of network strands of the macromers and chain pendants, k is the Boltzmann constant, and T is the absolute temperature. Calculation of the elastic modulus for this affine perfect networks yields G_e = 19 MPa, which satisfactorily overestimates the experimental measurement.

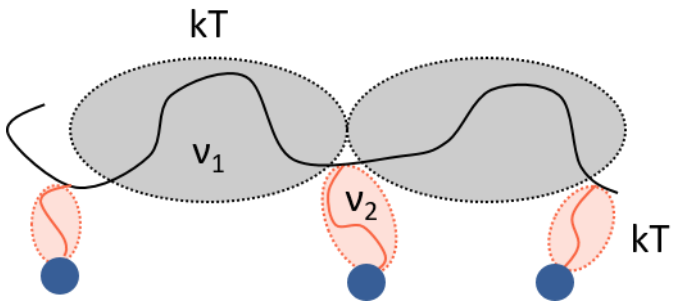

Figure S8: Chain pendants and macromers between IGE segments act as elastically active strands. Calculation within this affine perfect network framework yields an overestimated elastic modulus, consistent with the presence of both topological defects and imidazole ligands that do not form dynamic crosslinks based on metal-ligand coordination.

Linear Dielectric Response

Design Rules from Dilute Solution Theory

The ionic conductivity in PIGE-Ni^{2+} results from the presence of mobile ions in an electric field. Estimation of the equilibrium concentration of the various imidazole-Ni^{2+} species, together with inspection of the ionic conductivity, supports this assertion and provides a framework to illustrate design rules for high-performance materials. Though PIGE-Ni^{2+} is a polymer electrolyte where excluded volume interactions play a key role in ion transport, we consider it as a dilute liquid electrolyte to qualitatively reveal some critical features. The ionic conductivity, in the absence of concentration gradients, is then given by:

$$\sigma_{dc} = F^2(4u_{Ni}[Ni^{2+}] + u_{NTf2}[NTf_2^-])$$

Where F is the Faraday constant, u_{Ni} and u_{NTf2} the ionic mobilities, and $[Ni^{2+}]$ and $[NTf_2^-]$ the molar concentrations of free Ni^{2+} and NTf_2^-. This expression suggests that in the ion concentration regime investigated where $[NTf_2^-] \gg [Ni^{2+}]$, the majority of the current is expected to be carried by the NTf_2^- anions as a significant fraction of the Ni^{2+} cations are coordinated by imidazole and unable to move under an electrochemical potential gradient. Significant contributions of Ni^{2+} cations to the ionic current would require either the mobility of Ni^{2+} to be orders of magnitude larger than that of NTf_2^-, or an electrophilic polymer backbone that interacts strongly with NTf_2^-; both material design challenges similar to those posed for Li^+-conducting PEO-based polymers.[5] A more rigorous and quantitative assessment of ion transport in polymers has elegantly been discussed by Balsara et al.,[6] yet the simple discussion presented herein provides qualitative insights into ion transport and allows us to identify strategies to design novel ion-conducting polymers.

Role of Ionic Aggregation of the Ionic Mobility: The Continuum Approximation

Although excluded volume interactions couple the ion mobility to polymer segmental dynamics, it is still interesting to consider further the relationship between ionic conductivity, ion concentration, and ion mobility. In particular, upon addition of $Ni(NTf_2)_2$ to a PIGE of low dielectric constant there might be phase segregation at the nanometer length scale into ion-rich (*i.e.*, ionic aggregates) and ion-poor domains. These structural changes are expected to influence the bulk ionic conductivity because the chain dynamics, aggregate lifetimes, and ion contents are different in each domain; a characteristic feature of ion-containing polymers[7] recently addressed in a neat manner in a series of papers on precise poly(ethylene-*co*-acrylic acid) copolymers.[8] Though on a microscopic scale PIGE-Ni^{2+} networks might exhibit structural heterogeneities, these materials are assumed to exist as a continuum where they can be subdivided into infinitesimal elements with properties being those of the bulk material. Under this continuum approximation, there is a competition between ion concentration and ion mobility that dictates the bulk ionic conductivity.

References

1. Lee, B. F.; Wolffs, M.; Delaney, K. T.; Sprafke, J. K.; Leibfarth, F. A.; Hawker, C. J.; Lynd, N. A. Reactivity Ratios and Mechanistic Insight for Anionic Ring-Opening Copolymerization of Epoxides. *Macromolecules.* **2012,** 45 (9), 3722-3731.
2. Flory, P. J., *Principles of Polymer Chemistry*. Cornell University Press: Ithaca and London, 1953.
3. de Gennes, P.-G., *Scaling Concepts in Polymer Physics*. Cornell University Press: Ithaca and London, 1979.
4. Grindy, S. C.; Lenz, M.; Holten-Andersen, N. Engineering Elasticity and Relaxation Time in Metal-Coordinate Cross-Linked Hydrogels. *Macromolecules.* **2016,** 49 (21), 8306-8312.
5. Miller, T. F.; Wang, Z. G.; Coates, G. W.; Balsara, N. P. Designing Polymer Electrolytes for Safe and High Capacity Rechargeable Lithium Batteries. *Acc. Chem. Res.* **2017,** 50 (3), 590-593.
6. Balsara, N. P.; Newman, J. Relationship between Steady-State Current in Symmetric Cells and Transference Number of Electrolytes Comprising Univalent and Multivalent Ions. *J. Electrochem. Soc.* **2015,** 162 (14), A2720-A2722.

7. Eisenberg, A. Clustering of Ions in Organic Polymers. A Theoretical Approach. *Macromolecules.* **1970,** 3 (2), 147-154.
8. Middleton, L. R.; Winey, K. I. Nanoscale Aggregation in Acid- and Ion-Containing Polymers. *Annu. Rev. Chem. Biomol. Eng.* **2017,** 8 (1), 499-523.